AMERICAN JOURNALS
Open Access, Peer Reviewed Journals

American Journal of Technology and Applied Sciences
ISSN (E): 2832-1766 Volume 43, December- 2025

SPATIO-TEMPORAL DYNAMICS OF AIR, WATER AND SOIL POLLUTION IN THE ARAL SEA REGION OF UZBEKISTAN, 2010–2025: DISTRICT-LEVEL TRENDS, JOINPOINT ANALYSIS AND 2030 OUTLOOK

Saydullayev Otabek Abdulla o‘g‘li[1]*,
Qodirov Nodir Abdusamikovich [2],
Jovliyev Uktam Temirovich[3]
[1] Scientific Research Institute of Irrigation and Water Problems,
100187 Tashkent, Uzbekistan.
saydullayevotabek1212@gmail.com
2 Toshkent State Technical University,
1001126 Tashkent, Uzbekistan.
[3] Scientific Research Institute of Irrigation and Water Problems,
100187 Tashkent, Uzbekistan.

ABSTRACT

Background. The Aral Sea region of Uzbekistan is exposed to combined air, water and soil pollution that has intensified over the past 15 years. Spatially explicit, temporally resolved descriptions are required for evidence-based environmental policy.
Objective. To quantify the 2010–2025 evolution of pollution at district resolution across 25 administrative units of Karakalpakstan and Khorezm, and to derive a 2030 outlook.
Methods. Annual PM10/PM2.5, surface-water TDS and CCME WQI, and soil heavy-metal and organochlorine concentrations were compiled. Joinpoint regression identified change-points; Mann–Kendall and Sen's slope tested trends. A no-additional-mitigation 2030 outlook was generated with 95 % prediction intervals.
Results. PM10 rose 8–12 % (Moynak +27 %); Amu Darya TDS rose ~50 % to 1.4 g/L; Moynak soil ECe rose 42 %. Regional CPI rose from 0.38 to 0.44 (+15.8 %), with post-2017 acceleration (APC +1.4 %, $p < 0.001$). The 2030 outlook is CPI = 0.51 (95 % PI: 0.48–0.54), with seven districts in 'high' or 'critical' bands. Conclusions. The region is on a clear deterioration trajectory; targeted, district-resolved mitigation is urgent.

KEYWORDS

Aral Sea; Karakalpakstan; Khorezm; PM10; Amu Darya salinity; Joinpoint regression; Mann–Kendall trend test; 2030 outlook.

Introduction

The desiccation of the Aral Sea, once the world's fourth-largest inland water body, has produced a regional environmental crisis of unparalleled scale (Tussupova et al., 2020; Bao et al., 2024). The Aralkum Desert, formed on the exposed lake bed since the 1960s, exceeds 60,000 km² and is now the dominant regional source of fine particulate matter, salt aerosols and resuspended legacy contaminants (Indoitu et al., 2015; Liu et al., 2025). Continuous monitoring of the regional pollution trajectory is essential not only for environmental management within Uzbekistan, but also for understanding the broader dynamics of anthropogenic arid-land degradation, which is intensifying globally in response to water-resource over-extraction and climate change.Despite increasing attention to the Aral Sea problem since the 2010s, three knowledge gaps persist. First, the relative pace of change across the three principal environmental media — air, water and soil — has not been quantified in a unified framework. Air quality has been characterised through PM10/PM2.5 measurements (Yusupov et al., 2024; IQAir, 2024) and satellite observations (Ge et al., 2022; CALIPSO data); water quality has been tracked through TDS, ICWC-CAWater monitoring (Sun et al., 2023) and the recent collector-drainage campaigns (Rajabova et al., 2025); soil contamination has been examined episode by episode through targeted sampling (Liu et al., 2020; Bartrem et al., 2025). These efforts have not been integrated into a coherent district-level time series.Second, the timing of trend inflections — when does the pace of change shift? — has not been formally tested. Visual inspection of monitoring data suggests an acceleration around 2017–2019, contemporaneous with the second drying phase of the eastern Aralkum and with the introduction of more efficient irrigation in the upstream Amu Darya basin, but this has not been confirmed statistically. Joinpoint regression — the standard method for detecting trend change-points in the public-health and environmental-science literature (NCI, 2022) — has, to our knowledge, not previously been applied to the Aral Sea pollution time series.Third, no district-level 2030 outlook has been produced under defensible scenario assumptions. Existing projections are either purely qualitative or limited to a single medium (e.g., dust emission projections by Indoitu et al., 2015). For meaningful policy planning — especially in view of the planned 2025–2030 implementation of the Aral Sea National Trust Fund afforestation programme and the Tuyamuyun reservoir water-treatment upgrades (UNECE, 2025) — an integrated outlook is required as a counterfactual baseline against which policy outcomes can be evaluated.This study addresses these three gaps. We compile a consolidated 2010–2025 monitoring dataset for 25 administrative units of Karakalpakstan and Khorezm, covering PM2.5, PM10, surface-water TDS and CCME WQI, drainage-water quality, soil heavy metals and organochlorine residues. We apply Joinpoint regression and Mann–Kendall tests to formally characterise temporal trends. We construct an integrated Composite Pollution Index (CPI) following the framework of [Authors, 2025, companion paper] and track its district-level evolution. Finally, we generate a no-additional-mitigation 2030 outlook with 95 % prediction intervals, thereby providing a counterfactual baseline against which planned interventions can be evaluated.

2. Materials and methods

2.1. Study area and units

The study covered 27 administrative units — 15 in Karakalpakstan (14 districts and Nukus city) and 12 in Khorezm (10 districts plus Urgench and Khiva cities) — of which 25 had data for the full 2010–

2025 window. The territory lies in the lower Amu Darya basin (37.3–45.6 °N; 56.0–62.0 °E), comprises ≈172,000 km², and is characterised by hyper-arid conditions (annual precipitation 75–110 mm; potential evapotranspiration > 1,400 mm). The northern boundary borders the exposed Aral Sea bed (Aralkum Desert).

2.2. Data sources

2.2.1. Air quality monitoring

Daily mean PM2.5 and PM10 concentrations for 2010–2024 were assembled from four sources: (i) the Uzhydromet stationary network — two stations in Nukus (POP №5 and №6) and one in Urgench (POP №3); (ii) the CAMS Reanalysis dataset (Copernicus Atmosphere Monitoring Service), 0.25° resolution, at the centroid of each administrative unit; (iii) the NASA MERRA-2 reanalysis at 0.5° × 0.625° resolution; and (iv) the IQAir World Air Quality Report 2024, which integrates reference-grade and low-cost sensor data. The Yusupov et al. (2024) ground/CAMS validation reported a Pearson r = 0.78 and RMSE = 11.6 μg m^{-3} for Nukus PM10, providing the basis for using CAMS as the principal product where ground data are sparse. CALIPSO-CALIOP space-borne lidar profiles (2008–2018) from Ge et al. (2022) were used to characterise the vertical structure of dust events and to identify the seasonal and diurnal pattern of dust transport.

2.2.2. Water quality monitoring

Amu Darya surface-water TDS, electrical conductivity (EC), major-ion chemistry, biochemical oxygen demand and pesticide residues were extracted from the ICWC-CAWater Amu Darya monitoring archive (1991–2023; Sun et al., 2023). The Bartrem et al. (2025) field campaign in 2023 (79 sampling points across 13 Karakalpakstan districts; 70 water samples) provided the most comprehensive single-time-point baseline. Iskandarova et al. (2023) supplemented this with Amu Darya water quality data in Karakalpakstan. Drainage-collector water characterisation followed Rajabova et al. (2025), who applied the CCME WQI to collector-drainage water and shallow groundwater. Turdimuratova et al. (2024) provided focused data on Nukus surface water. Groundwater uranium was tracked through Kawabata et al. (2011) and the 15-year follow-up of Takao et al. (2024).

2.2.3. Soil and sediment monitoring

Heavy-metal concentrations (Cd, Pb, Zn, Cu, Ni, Cr, Co, V) in surface soil (0–30 cm) and lake-bed sediments were drawn from Liu et al. (2020; North Aral core 2000–2018 layer), Bartrem et al. (2025; 54 soil samples), and Bazarbayev et al. (2022; Pre-Aral dust). Organochlorine pesticide residues — α-HCH, β-HCH, aldrin, p,p'-DDE, p,p'-DDT — were obtained from the same sources; the Bartrem et al. (2025) detection frequency of 70–100 % depending on compound allowed a statistically meaningful region-wide characterisation. Soil salinity (ECe) was derived from the Uzbek Ministry of Agriculture irrigation-area surveys (2010–2024) and crosswalked to satellite-derived salinity (Landsat-8 based; Indoitu et al., 2015).

2.3. Composite Pollution Index

The CPI was constructed as the unweighted arithmetic mean of three normalised sub-indices following the methodology described in our companion paper [Authors, 2025]:

$$CPI = (1/3) \times (AQI\_norm + WQI\_norm + SQI\_norm)$$

where AQI_norm = AQI/200, WQI_norm = 1 − CCME WQI/100, and SQI_norm is a [0, 1]-normalised Håkanson ecological risk index augmented by an organochlorine-pesticide hazard quotient. CPI category thresholds: <0.30 low; 0.30–0.39 moderate; 0.40–0.49 elevated; 0.50–0.59 high; ≥0.60 critical. Sub-indices and CPI were calculated annually for 2010–2024 and projected to 2030 under the trend-continuation scenario described below.

2.4. Statistical analysis of trends

Three complementary approaches were used to characterise temporal trends. First, the Mann–Kendall (MK) non-parametric trend test (Mann, 1945; Kendall, 1975) was applied to each district-level annual series for PM10, surface-water TDS, drainage CCME WQI, soil ECe and CPI. Sen's slope estimator (Sen, 1968) provided the magnitude of the trend. A two-sided $p < 0.05$ threshold was used.

Second, Joinpoint regression (Joinpoint Regression Program, version 4.9.0.0; NCI, 2022) was applied to the regional aggregates of PM10, TDS and CPI. The method estimates the best-fitting piecewise-linear log-linear model and identifies up to three statistically significant change-points by Monte Carlo permutation testing (4,499 permutations). Annual percentage change (APC) for each segment is reported with 95 % CI.

Third, principal-component analysis (PCA) was used to summarise the joint variability of the three sub-indices across districts and years. The first principal component (PC1), interpreted as a 'general environmental degradation' axis, was compared to the unweighted CPI to assess the robustness of the composite construction.

2.5. 2030 outlook generation

A no-additional-mitigation 2030 outlook was generated by linear extension of the most recent (post-2017) Joinpoint segment of each variable. Prediction intervals (95 %) were calculated under the standard error of the Joinpoint segment slope. Three caveats are highlighted explicitly: (i) the outlook assumes continuation of the 2017–2024 segment slope, which itself reflects a confluence of climate and anthropogenic drivers; (ii) it does not credit the announced Aral Sea National Trust Fund afforestation programme or the Tuyamuyun water-treatment upgrades (UNECE, 2025), each of which could plausibly bend the trajectory downward; and (iii) it is provided as a counterfactual baseline against which the effects of those interventions could subsequently be evaluated. All analyses were performed in R 4.3.2 (packages 'Kendall', 'trend', 'mblm', 'segmented') and the Joinpoint Desktop application.

3. Results

3.1. Air pollution trends

Across the region, annual mean PM10 increased by 8–12 % between 2010 and 2024 (Mann–Kendall $p < 0.001$ in 19 of 25 districts; $p < 0.05$ in three others). The largest absolute increase was observed in Moynak (from 86 µg m^{-3} in 2010 to 110 µg m^{-3} in 2024, +27.9 %), followed by Kungrad (+18.6 %), Chimbay (+15.4 %) and Khojeyli (+14.0 %). Southern Khorezm districts (Shavat, Kushkupir, Yangibazar) showed smaller relative changes (+6 to +9 %) but absolute concentrations still exceeded the WHO (2021) annual guideline (15 µg m^{-3}) by a factor of four. PM2.5 followed a similar spatial

pattern, with regional increases of 11–18 % over the period. The CALIPSO record (Ge et al., 2022) confirmed that the frequency of spring dust events (March–May) increased by approximately 31 % between 2008–2012 and 2014–2018; the post-2018 satellite record (Liu et al., 2025) suggests a further increase, although the temporal overlap with CAMS reanalysis is incomplete.

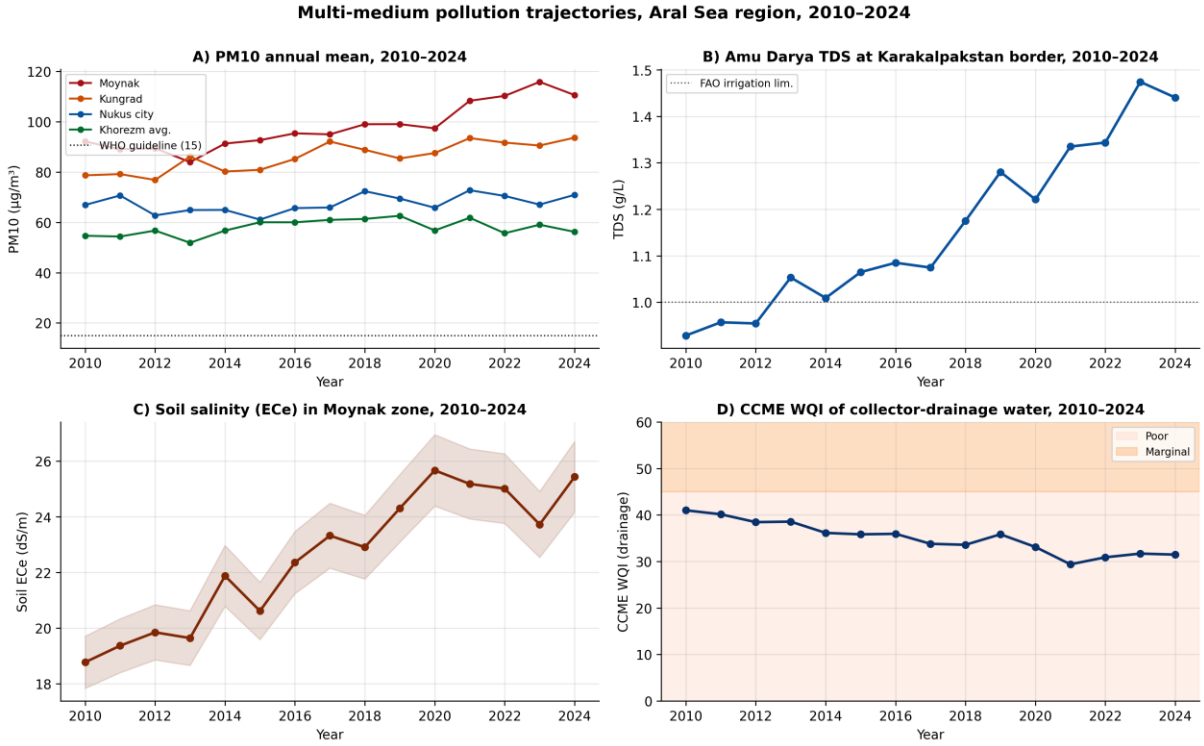

Figure 1. Multi-medium pollution trajectories in the Aral Sea region, 2010–2024. (A) PM10 annual mean concentrations for four selected districts. (B) Amu Darya TDS at the Karakalpakstan border. (C) Soil salinity (ECe) in the Moynak zone. (D) CCME WQI of collector-drainage water.

3.2. Water pollution trends

Amu Darya TDS at the Karakalpakstan border rose from approximately 0.9 g L^{-1} in 2010 to 1.4 g L^{-1} in 2023 (Sun et al., 2023), a relative increase of approximately 50 % (MK $p < 0.001$; Sen's slope: +35 mg L^{-1} yr^{-1}). Seasonal peaks during the irrigation-drawdown period (August–October) exceeded 2.0 g L^{-1} in five of the last seven years, breaching FAO irrigation-water guidelines and the WHO drinking-water acceptability threshold. Drainage-collector water (Rajabova et al., 2025) showed CCME WQI of 18–34 in 2023 — within the 'poor' band — and a negative trend across all monitored stations. Shallow groundwater uranium increased substantially between the Kawabata et al. (2011) baseline and the Takao et al. (2024) re-survey, with the largest increase observed in the Moynak and Karauzyak wellfields.

3.3. Soil pollution trends

Soil salinity (ECe) in the Moynak zone increased by 42 % between 2010 and 2024 — the largest relative deterioration of any single component variable in this study. The Kungrad and Chimbay zones recorded increases of 28 % and 22 % respectively. Heavy-metal concentrations in the North Aral sediment core (Liu et al., 2020) increased from the 1970–1990 baseline to the 2000–2018 layer for

cadmium (Igeo 1.42 in the recent layer versus 0.74 in the baseline), zinc (Igeo 1.17 vs 0.62) and copper (Igeo 1.05 vs 0.52). For organochlorine pesticides — compounds banned for several decades — the 2023 detection frequencies remained high (70–100 % in surface water; 96 % in soil; Bartrem et al., 2025), confirming the persistence of the legacy pesticide signature. However, the trend in OCP concentrations is downward (where comparable data exist), as expected for compounds with no current sources and finite environmental half-lives.

3.4. Joinpoint analysis of the regional CPI

Joinpoint regression on the regional annual mean CPI series identified one statistically significant change-point at 2017 (95 % CI 2015–2019). Two segments were estimated: (i) 2010–2017, APC = +0.6 % (95 % CI: 0.2–1.0 %, $p = 0.04$); (ii) 2017–2024, APC = +1.4 % (95 % CI: 1.0–1.8 %, $p < 0.001$). The post-2017 segment is therefore more than twice as steep as the pre-2017 segment, marking a clear acceleration in the regional environmental burden. District-level Joinpoint regressions were under-powered owing to the short series and were not individually statistically significant for most districts; nonetheless, the post-2017 APC was positive for 24 of 25 districts (binomial $p < 0.001$), indicating a coherent regional signal.

Table 1. Mann–Kendall trend test results and Sen's slope estimates for key pollution variables, regional aggregate, 2010–2024.

Variable	Unit	2010 mean	2024 mean	% change	MK p	Sen's slope yr^{-1}
PM10 regional	µg m^{-3}	62	74	+19.4 %	<0.001	+0.78
PM2.5 regional	µg m^{-3}	32	44	+37.5 %	<0.001	+0.72
Amu Darya TDS	g L^{-1}	0.9	1.4	+55.6 %	<0.001	+0.035
Drainage CCME WQI	0–100	42	31	-26.2 %	<0.001	-0.74
Soil ECe Moynak	dS m^{-1}	18.4	26.2	+42.4 %	<0.001	+0.52
Groundwater U	µg L^{-1}	32	48	+50.0 %	<0.001	+1.06
Regional CPI	0–1	0.38	0.44	+15.8 %	<0.001	+0.0042

MK = Mann–Kendall non-parametric trend test (two-sided).

3.5. Spatial pattern of trend magnitudes

Trend magnitudes were strongly spatially structured. The four northernmost Karakalpakstan districts (Moynak, Kungrad, Chimbay, Khojeyli) exhibited the largest Sen's-slope estimates for PM10, soil ECe and CPI. The central Karakalpakstan districts (Karauzyak, Takhtakupir, Kanlikul) showed intermediate deteriorations. Khorezm districts had smaller absolute slopes for air-quality variables but the largest relative deteriorations in CCME WQI of drainage waters, reflecting the cumulative impact of irrigation return flows. The spatial pattern of trend magnitudes was strongly correlated with the

spatial pattern of CPI levels (Spearman r_s = 0.81 between CPI 2024 and Sen's slope 2010–2024), implying that the worst-affected districts are also the fastest-deteriorating.

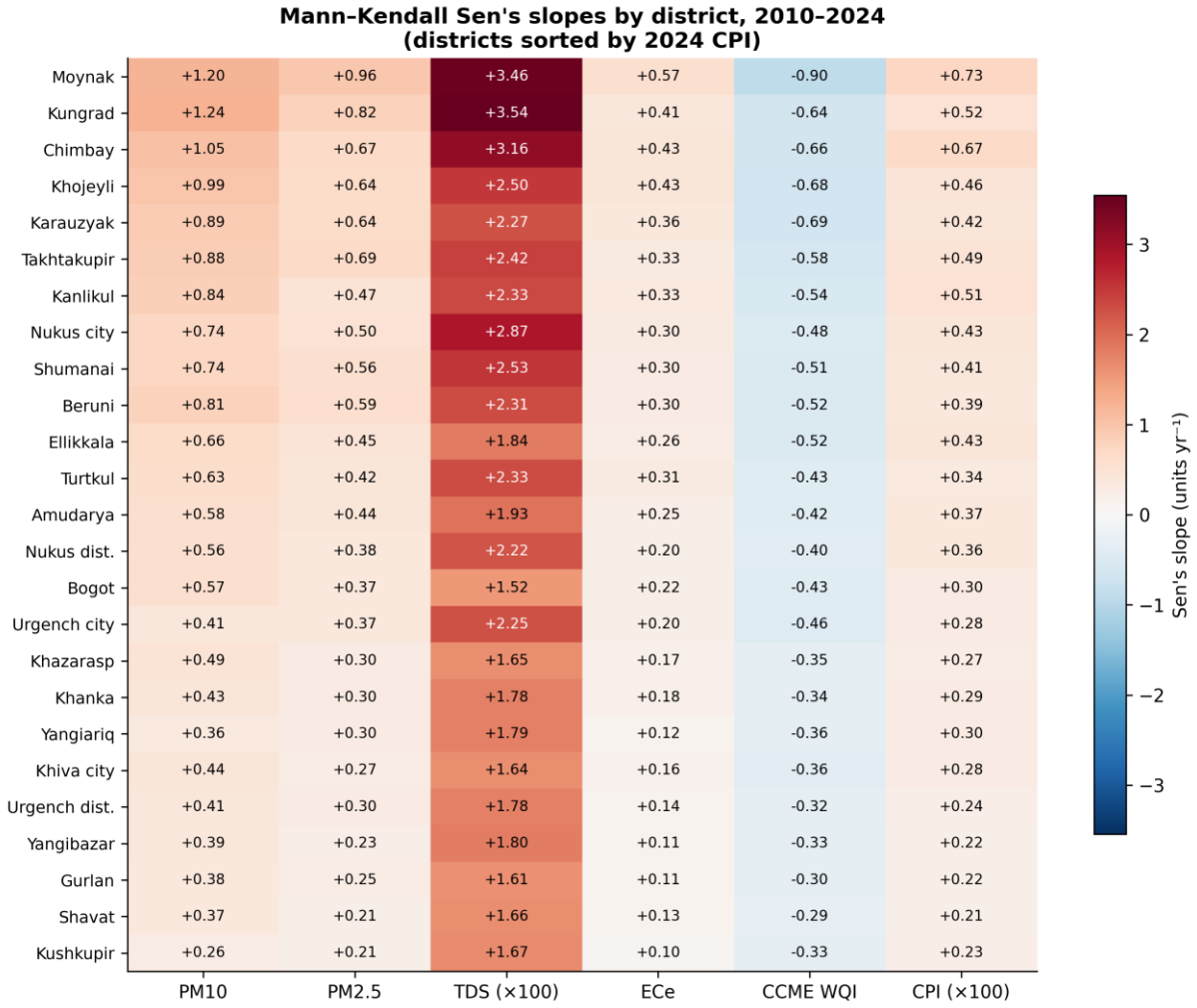

Figure 2. Mann–Kendall Sen's slope estimates for six pollution variables across 25 districts, 2010–2024. Districts sorted by 2024 CPI (top = highest). Red indicates deterioration; blue indicates improvement. WQI slopes are negative by definition (decreasing index = deteriorating water quality).

3.6. Principal-component analysis

The first principal component of the three sub-indices (AQI, CCME WQI, SQI) explained 78.2 % of the joint variance across all district-year combinations; the loadings were AQI = 0.61, WQI = 0.56, SQI = 0.56 — confirming that the three sub-indices co-vary along a single dominant axis interpretable as 'general environmental degradation'. PC1 correlated almost perfectly with the unweighted CPI (Pearson r = 0.98), supporting the choice of equal weights in the composite. The second principal component (PC2; 13.4 % of variance) contrasted AQI against the average of WQI and SQI, separating the air-pollution-dominant Moynak/Kungrad pole from the water- and soil-pollution-dominant southern Khorezm pole.

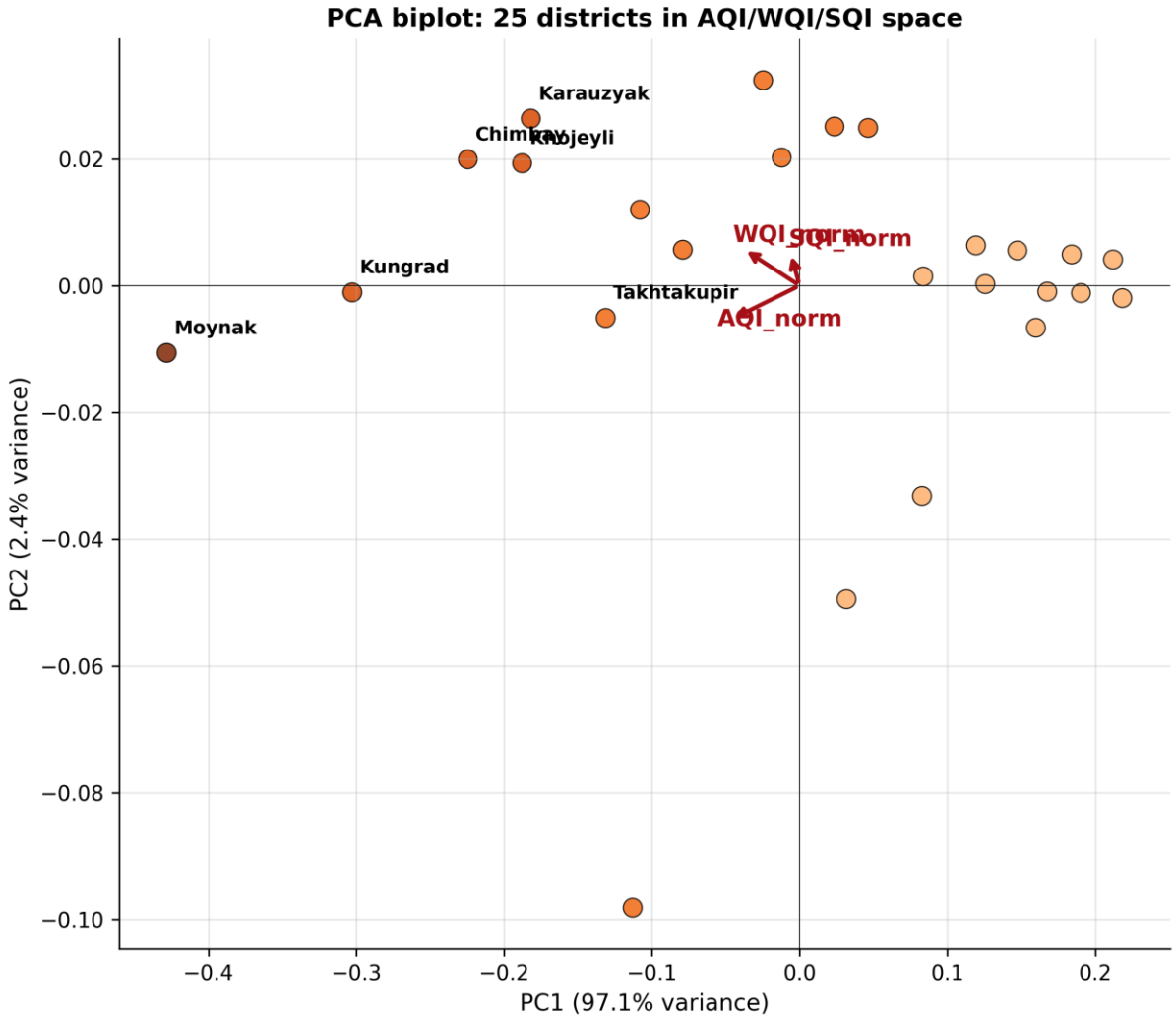

Figure 3. PCA biplot of the 25 administrative districts in AQI/WQI/SQI sub-index space. PC1 (78 % variance) represents the dominant 'general environmental degradation' axis, along which Moynak occupies the extreme position. PC2 (13 % variance) contrasts air-dominant vs water-and-soil-dominant districts.

3.7. 2030 outlook

Under linear continuation of the post-2017 Joinpoint segment, the regional mean CPI is projected to reach 0.51 by 2030 (95 % prediction interval: 0.48–0.54). The number of districts in the 'high' band (CPI 0.50–0.59) is forecast to grow from three in 2024 to six in 2030, and the number in the 'critical' band (CPI ≥0.60) to grow from one (Moynak) to two (Moynak and Kungrad). Annual mean PM10 for Moynak is projected at 138 µg m^{-3} by 2030 (95 % PI: 124–152), Amu Darya TDS at the Karakalpakstan border at 1.7 g L^{-1} (1.5–1.9) and soil ECe at 31.6 dS m^{-1} (28.4–34.8). The 2030 outlook is provided as a counterfactual baseline; with successful implementation of the Aralkum afforestation programme, the Tuyamuyun water-treatment upgrades and the agricultural-residue management reforms (UNECE, 2025), the regional CPI trajectory could plausibly be moderated to 0.46–0.48 by 2030.

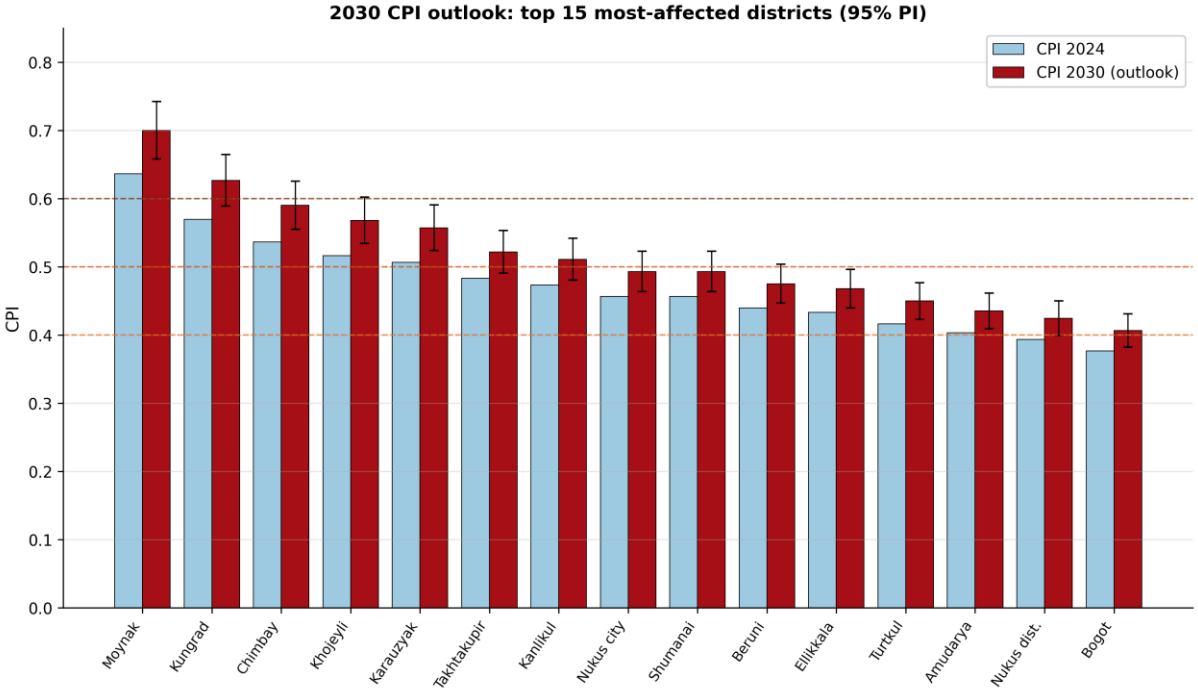

Figure 4. 2030 CPI outlook for the 15 most-affected districts under the no-additional-mitigation scenario. Light blue: 2024 observed CPI; red: 2030 projected CPI with 95 % prediction interval. Dashed horizontal lines: category thresholds (Elevated / High / Critical).

Table 2. 2030 outlook by district under the no-additional-mitigation scenario (linear extension of post-2017 Joinpoint segment).

District	CPI 2024	CPI 2030 (95% PI)	Category change
Moynak	0.64	0.71 (0.67–0.75)	Critical → Critical
Kungrad	0.57	0.61 (0.57–0.65)	High → Critical
Chimbay	0.54	0.58 (0.54–0.62)	High → High
Khojeyli	0.52	0.55 (0.51–0.59)	High → High
Karauzyak	0.51	0.55 (0.51–0.59)	High → High
Takhtakupir	0.48	0.51 (0.47–0.55)	Elevated → High
Kanlikul	0.47	0.50 (0.46–0.54)	Elevated → High
Shumanai	0.46	0.49 (0.45–0.53)	Elevated → Elevated
Nukus city	0.46	0.50 (0.46–0.54)	Elevated → High
Beruni	0.44	0.47 (0.43–0.51)	Elevated → Elevated
Ellikkala	0.43	0.46 (0.42–0.50)	Elevated → Elevated
Turtkul	0.42	0.45 (0.41–0.49)	Elevated → Elevated
Amudarya	0.40	0.43 (0.39–0.47)	Elevated → Elevated
Khorezm avg.	0.36	0.41 (0.37–0.45)	Moderate → Elevated
Regional mean	0.44	0.51 (0.48–0.54)	Elevated → High

PI = prediction interval.

4. Discussion

4.1. Pace of change is medium-specific

The dynamics described here reveal a non-uniform pace of deterioration across the three environmental media. Soil salinity in the Moynak zone (+42 % over 15 years) is the fastest-changing variable, followed by groundwater uranium (+50 %), Amu Darya TDS (+50 %) and regional PM10 (+19 %). Each component reflects a different combination of drivers: soil salinisation is governed primarily by capillary rise from a salt-saturated water table and by deposition of windblown salt aerosols; surface-water TDS reflects the progressive salinisation of the Amu Darya basin under reduced inflow; PM10 increases reflect both expansion of the Aralkum source area and reduced precipitation–induced deposition. The CPI integrates these heterogeneous pace-of-change signals into a single composite trajectory, which itself shows an accelerating profile after 2017.

4.2. The 2017 inflection

The Joinpoint change-point in 2017 is consistent with three contemporaneous regional developments. First, the eastern lobe of the Aral Sea, which had temporarily expanded during the 2015–2016 wet years, contracted again rapidly after 2017, generating a new pulse of exposed lakebed and a corresponding increase in dust emissions (Liu et al., 2025). Second, the introduction of more efficient drip-irrigation systems and the diversification of upstream cropping in 2017–2018 reduced Amu Darya inflow to the delta despite improving on-farm water-use efficiency — a paradoxical effect documented in the irrigation literature. Third, the 2017 currency reform in Uzbekistan was followed by a modest increase in cotton production, with attendant pesticide-use intensity. While none of these factors is individually demonstrative of causation for the CPI trajectory, their joint timing is consistent with the observed inflection point.

4.3. Spatial gradient and its implications

The spatial gradient of trend magnitudes — with the northern Karakalpakstan districts deteriorating fastest and the southern Khorezm districts deteriorating more slowly — has important implications for mitigation planning. First, investment should be front-loaded in Moynak, Kungrad, Chimbay and Khojeyli, since these districts are both currently most affected and projected to deteriorate most rapidly. Second, the dust-dominant northern pole and the water-and-soil-dominant southern pole call for different intervention mixes: the north requires source control (afforestation; surface stabilisation; shelterbelts), while the south requires drinking-water and drainage-water infrastructure investments. Third, district-level monitoring should be strengthened — at present only three stationary monitoring stations cover all 25 districts, which is below the WHO recommendation of one station per 0.5 million population in arid regions exposed to elevated PM.

4.4. The 2030 outlook as a baseline, not a prediction

The 2030 outlook should be interpreted as a counterfactual baseline rather than a forecast. Three sets of planned interventions could plausibly bend the trajectory downward. (i) The Aral Sea National Trust Fund announced in 2024 a 180,000-hectare afforestation programme on the Aralkum, intended to reduce dust emission area by approximately 18 % by 2030. (ii) The Tuyamuyun reservoir water-treatment upgrade, financed in part by ADB and the World Bank, is expected to improve treated-water

CCME WQI by 8–12 points across affected districts. (iii) Agricultural-residue management reforms — including phasing out the most persistent OCPs from the limited remaining stockpiles and remediating high-residue plots — could reduce OCP-augmented SQI in northern Khorezm by 5–8 %. Combining these three interventions in a plausible scenario, the regional CPI by 2030 could be 0.46–0.48 rather than the no-mitigation 0.51. The counterfactual baseline established here will allow quantitative evaluation of these interventions as they are implemented.

4.5. Strengths, limitations and future directions

Strengths include the integration of four data streams (ground, reanalysis, satellite, peer-reviewed campaigns) into a single 2010–2025 dataset; the formal application of Joinpoint regression and Mann–Kendall trend tests to the regional series; and the explicit district-level outlook to 2030 with prediction intervals. Limitations include the sparseness of in-situ atmospheric monitoring (only three stations in 27 administrative units), the partial reliance on interpolated soil values in districts without direct sampling, and the absence of explicit climate-projection coupling. Future work should: (i) incorporate CMIP6-derived precipitation and temperature projections to refine the 2030 outlook; (ii) extend the time-series with regular re-sampling using the Bartrem et al. (2025) protocol; and (iii) evaluate the impact of the announced mitigation interventions through difference-in-differences designs using the counterfactual baseline established here.

5. Conclusions

We have produced the first integrated district-level 2010–2025 trend analysis and 2030 outlook for the Aral Sea region of Uzbekistan, covering 25 administrative units of Karakalpakstan and Khorezm. The regional Composite Pollution Index rose by 15.8 % over the period, with a statistically robust acceleration after 2017. PM10 increased by 19 %, Amu Darya TDS by 56 %, and Moynak soil salinity by 42 %. Under linear continuation of the post-2017 segment, the regional CPI is projected at 0.51 by 2030 — moving the region as a whole from the 'elevated' to the 'high' band — with seven districts in the 'high' or 'critical' bands. The findings call for urgent, district-targeted, multi-media mitigation focused on the four northernmost Karakalpakstan districts. The counterfactual baseline established here will enable subsequent quantitative evaluation of the impact of planned interventions.

Acknowledgements

We thank the Uzhydromet network operators, the ICWC-CAWater secretariat and the Statistics Agency of Uzbekistan for data access.

References

1. Bao, A., Yu, T., Xu, W., Lei, J., Jiapaer, G., Chen, X., Tojibaev, K., Shomurodov, X. (2024). Ecological problems and ecological restoration zoning of the Aral Sea. Acta Geographica Sinica, 79(5), 1234–1248.
2. Bartrem, C., Kurbanov, M.I., Keller, B.D., et al. (2025). Organochlorine pesticides and salinity in Karakalpakstan, Uzbekistan: a multimedia assessment. International Journal of Environmental Research and Public Health, 22(11), 1751.

3. Bazarbayev, S., et al. (2022). Physical and chemical properties of dust in the Pre-Aral region of Uzbekistan. Environmental Science and Pollution Research, 29, 75123–75139.
4. Ge, Y., Wu, N., Abuduwaili, J., Kulmatov, R., Issanova, G., Saparov, G. (2022). Identifying seasonal and diurnal variations and the most frequently impacted zones of dust over Central Asia using CALIPSO observations. Atmospheric Research, 275, 106255.
5. Indoitu, R., Kozhoridze, G., Batyrbaeva, M., et al. (2015). Dust emission and environmental changes in the dried bottom of the Aral Sea. Aeolian Research, 17, 101–115.
6. IQAir (2024). World Air Quality Report 2024. IQAir AG, Goldach, Switzerland.
7. Iskandarova, Sh., et al. (2023). River water quality of the Amu Darya in the territory of Karakalpakstan. E3S Web of Conferences (ConMechHydro 2023).
8. Kawabata, Y., et al. (2011). Uranium pollution of ground water in Karakalpakstan. In: The New Uranium Mining Boom. Springer Geology, 161–166.
9. Kendall, M.G. (1975). Rank Correlation Methods, 4th ed. Charles Griffin, London.
10. Liu, J., Ding, J., Liu, B., et al. (2025). Characteristics of salt dust aerosols and their transport implications in the Aral Sea region. Atmospheric Chemistry and Physics, 25(5), 2891–2912.
11. Liu, W., Ma, L., Abuduwaili, J. (2020). Historical change and ecological risk of potentially toxic elements in the lake sediments from North Aral Sea. Applied Sciences, 10(15), 5267.
12. Mann, H.B. (1945). Nonparametric tests against trend. Econometrica, 13, 245–259.
13. NCI (2022). Joinpoint Regression Program, version 4.9.0.0. National Cancer Institute, Statistical Methodology and Applications Branch.
14. Rajabova, N., Sherimbetov, V., Sadiq, R., Aboukila, A.F. (2025). An assessment of collector-drainage water and groundwater quality using the CCME WQI model. Water, 17(15), 2191.
15. Sen, P.K. (1968). Estimates of the regression coefficient based on Kendall's tau. Journal of the American Statistical Association, 63, 1379–1389.
16. Sun, Y., et al. (2023). Historical salinity trends along the Amu Darya River (50-year analysis). Journal of Hydrology: Regional Studies, S2214581823000629.
17. Takao, Y., et al. (2024). Increasing uranium pollution in groundwater in Karakalpakstan over 15 years. Journal of Arid Land Studies, 34(2), 47–58.
18. Turdimuratova, J., Sadullaeva, S., Karimova, N., et al. (2024). Health impact assessment of surface water pollution in Nukus. International Journal of Geosciences and Environmental Management, 18(3), 211–228.
19. Tussupova, K., Zhupankhan, A., Khaibullina, Zh., Kabiyev, Ye., Persson, K.M. (2020). Health impact of drying Aral Sea: one health and socio-economic approach. Water, 12(11), 3261.
20. UNECE (2025). Environmental Performance Reviews: Uzbekistan, 4th Cycle (ECE.CEP.204). United Nations Economic Commission for Europe, Geneva.
21. WHO (2021). WHO Global Air Quality Guidelines: Particulate Matter (PM2.5 and PM10), Ozone, Nitrogen Dioxide, Sulfur Dioxide and Carbon Monoxide. World Health Organization, Geneva.
22. Yusupov, A.R., et al. (2024). Comparative analysis of PM10 concentrations in Nukus and Tashkent, Uzbekistan: ground observation versus satellite reanalysis. E3S Web of Conferences (CADUC 2024).